CHEMISTRY OF MATERIALS

ARTICLE

pubs.acs.org/cm

Harmonizing Triplet Level and Ambipolar Characteristics of Wide-Gap Phosphine Oxide Hosts toward Highly Efficient and Low Driving Voltage Blue and Green PHOLEDs: An Effective Strategy Based on Spiro-Systems

Jie Zhao,[†,‡] Guo-Hua Xie,[§,‡] Cheng-Rong Yin,[⊥] Ling-Hai Xie,[⊥] Chun-Miao Han,[†] Run-Feng Chen,[⊥] Hui Xu,[*,†] Ming-Dong Yi,[⊥] Zhao-Peng Deng,[†] Shu-Fen Chen,[⊥] Yi Zhao,[*,§] Shi-Yong Liu,[§] and Wei Huang[*,⊥]

[†]Key Laboratory of Functional Inorganic Material Chemistry, Ministry of Education, Heilongjiang University, 74 Xuefu Road, Harbin 150080, China

[⊥]Key Laboratory for Organic Electronics & Information Displays (KLOEID), Institute of Advanced Materials (IAM), Nanjing University of Posts & Telecommunications, 9 Wenyuan Road, Nanjing 210046, China

[§]State Key Laboratory on Integrated Optoelectronics, College of Electronics Science and Engineering, Jilin University, 2699 Qianjin Street, Changchun 130012, China

Supporting Information

ABSTRACT: A series of phosphine oxide (PO) hosts based on diphenylphosphine oxide and spiro[fluorene-9,9′-xanthene] (SFX) moieties, SFX2PO, SFX27PO, SFX2′PO, and SFX2′7′PO, were designed and synthesized. On the basis of the different electrical properties of xanthene and fluorene in SFX, the influence of substitution position on the chemical and optophysical properties of the ambipolar-core based systems were investigated in detail. The effective strategy of introducing electron-withdrawing PO moieties in electron-deficient moieties in the molecules accompanied with suitable linkages insulating the electron-rich and -deficient moieties was convincingly demonstrated, which can endow the hosts with much better carrier injecting and transporting ability and high enough T_1 for blue and green phosphors. As the results, the operating voltages of the devices based on SFX2PO and SFX27PO were much lower than those of the devices based on SFX2′PO and SFX2′7′PO. Simultaneously, the efficiencies of the SFX2PO based devices were about twice of those of the devices based on SFX2′PO and SFX2′7′PO. We suppose that it is not necessary to achieve too high T1 and improved electron injection through PO moieties at the cost of sacrificing the hole injecting ability of the chromophores. An ideal strategy is preserving high enough T1 and improving electron injection by utilizing PO moieties without reducing hole injection and transportation in the hosts.

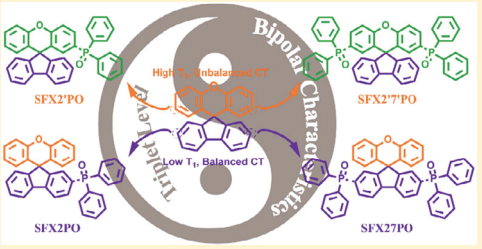

KEYWORDS: phosphine oxide, electrophosphorescence, spiro-compounds, host, substitution effect

INTRODUCTION

The highly efficient phosphorescent organic light-emitting diodes (PHOLEDs) were focused on in recent year because of their preeminent characteristics, such as harvesting both singlet and triplet excitons, and wide applications in the fields of displays and solid-state lighting sources.[1] Although PHOLEDs could potentially approach nearly 100% internal quantum efficiency, the longer lifetimes of triplet excitons commonly induce the worse multiparticle annihilation, which seriously reduces the real efficiencies of these electrophosphorescent devices.[2] To restrain the concentration quenching and triplet−triplet annihilation (TTA), the phosphors are dispersed in some matrixes so as to limit their intermolecular interaction.[3] Among the common approaches, the doping/blending systems have been paid much attention and it has been realized that most of the highest efficient PHOLEDs consist of carrier-transporting hosts and phosphorescent (PH) dyes in the emission layers (EMLs).[2] Nevertheless, the stable and efficient blue-emitting PHOLEDs are still significant challenges.

The high triplet excited level (T_1, ~3.0 eV) and excellent carrier injecting/transporting ability are two essential conditions for efficient hosts used in blue-emitting PHOLEDs,[4] which are actually contradictory to each other, since the former requires the small conjugated length, whereas the larger conjugated group benefits the latter. Therefore, the small molecules with considerable carrier transporting ability and high T_1, such as carbazole,[5] fluorene,[6] and dibenzofuran,[7a] are used as the chromophores to construct hosts by the incorporation of meso, twisted, or insulating linkage[5−8] to reduce the influence of the modification on the excited energy levels and simultaneously improve the stability and compatibility. Nevertheless, it is shown that the hosts based

Received: June 11, 2011
Revised: October 1, 2011
Published: November 18, 2011

Scheme 1. Molecular Structures of the Spiro-PO Compounds

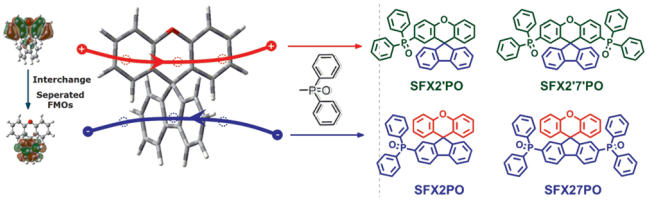

on these kinds of structures (such as N,N′-dicarbazolyl-3,5-benzene (mCP),[5a] 4,4′-bis(9-carbazolyl)-2,2′-dimethyl-biphenyl (CDBP),[5b] and diphenyl-di(o-tolyl)-silane (UGH1)[8]) can not supply satisfied carrier injecting/transporting ability in EMLs and subsequently result in high driving voltage. Recently, the phosphine oxide (PO) hosts in which the insulating P═O moieties can efficiently polarize the molecules because of their electron-withdrawing effect became attractive.[7,9] Therefore, the introduction of P═O moieties facilitates the formation of efficient hosts with high T_1 and ambipolar injecting/transporting ability on the basis of hole-transporting chromophores (e.g., carbazole) and electron-transporting PO groups (e.g., diphenylphosphine oxide (DPPO)). Lee[10] and Cheng[11] report several PO hosts with the structures of DPPO-bonding carbazole derivatives for which the excellent current−voltage ($I-V$) characteristics and highly efficient deep-blue electrophosphorescence are realized. Nevertheless, it is noticeable that the direct linkage of DPPO and carbazole induces the lowest unoccupied molecular orbital (LUMO) and the highest occupied molecular orbital (HOMO) to fall down simultaneously. As a result, the electron injecting/transporting ability of the hosts remarkably becomes strong, but at the same time, it weakens their hole injecting/transporting ability. Therefore, for constructing the hosts with the balanced carrier injecting/transporting ability, it is still a great challenge to realize the balance between preserving a sufficiently high T_1 of the chormophores and improving/inheriting the carrier injecting/transporting ability through P═O moieties.

Recently, we reported several fluorene-based PO hosts according to the strategy of indirect linkage.[12] It is shown that DPPO moieties substituted at the 9 position of fluorene hardly influence the frontier molecular orbitals (FMOs). Considering the widely investigation of the double-channel characteristics of the spiro-compounds, this gave us a revelation that the efficient PO hosts with improved and balanced carrier injecting/transporting can be realized through reasonable modification of suitable chromophores with spiro-structure. In our former work,[13] a suitable spiro-compound spiro[fluorene-9,9′-xanthene] (SFX) was proved as a bipolar molecule with separated FMOs (Scheme 1). The independent and different physical properties of the fluorene and xanthene moieties make it feasible to finely tune the carrier injecting/transporting ability.

In this contribution, DPPO moieties were introduced at 2,7-positions of fluorene in SFX to form two spiro-PO hosts, biphenyl (Spiro[fluorene-9,9′-xanthen]-2-yl) phosphine oxide (SFX2PO) and Spiro[fluorene-9,9′-xanthene]-2,7-diyl-bis(biphenylphosphine oxide) (SFX27PO). Simultaneously, other two spiro-PO compounds formed by substitution at 2′,7′-position of xanthene of SFX were also synthesized for comparison, which were named biphenyl (spiro [fluorene-9,9′-xanthen]-2′-yl)phosphine oxide (SFX2′PO) and spiro [fluorene-9,9′-xanthene]-2′,7′-diyl-bis (diphenylphosphine oxide) (SFX2′7′PO), respectively (Scheme 1). The influence of the DPPO-substitution at different moieties of SFX (fluorene or xanthene) on the chemical and optophysical properties of the corresponding compounds was investigated. Highly efficient blue and green emitting PHOLEDs with low driving voltages (4.4 and 3.3 V at ∼1000 cd m^2, respectively) and reduced efficiency roll-offs were demonstrated.

EXPERIMENTAL SECTION

Materials and Instruments. *n*-Butyllithium (*n*-BuLi), 4-bromo phenol, 9-fluorenone, and chlorodiphenylphosphine were obtained from J&K Chem. Co. and were used without further purification. 2-Bromospiro[fluorene-9,9′-xanthene] and 2,7-dibromospiro[fluorene-9,9′-xanthene] were obtained from Nanjing Fountain Global Display Technologies Co.,Ltd. Tetrahydrofuran (THF) was distilled over sodium, and air-sensitive reagents were handled in an atmosphere of dry N_2.

^{1}H NMR in $CDCl_3$ was recorded at 400 MHz using a Varian Mercury 400 plus spectrometer. The mass spectrometry was performed using a Gas Chromatograph Mass Spectrometer (SHIMADZU QP2010 Plus). For the MALDI-TOF MS spectra, the spectra were recorded in reflective mode without addition of any substrate. Melting points were determined by a Fukai (Beijing) X-4 digital melting point instrument. Absorption spectra were measured with a Shimadzu UV-3150 spectrometer and emission spectra were recorded on a Shimadzu RF-530XPC luminescence spectrometer. Differential scanning calorimetry (DSC) analyses were performed on a Shimadzu DSC-60A Instrument. Thermogravimetric analyses (TGA) were conducted on a Shimadzu DTG-60H thermogravimetric Analyzer under a heating rate of 10 °C/min and a nitrogen flow rate of 50 cm^3/min. Cyclic voltammetric (CV) studies were conducted using an CHI600C in a typical three-electrode cell with a platinum sheet working electrode, a platinum wire counter electrode, and a silver/silver nitrate (Ag/Ag^+) reference electrode. Ultraviolet photoelectron spectra (UPS) measurements were carried out with a Shimadzu/Kratos Axis Ultra DLD spectrometer, using the HeI radiation (21.21 eV) from a He discharge lamp. Peaks were recorded with the constant pass energy of 5 eV and the step size of 0.05 eV. The pressure in the analysis chamber was around 4.3×10^{-9} Torr. The instrument was operated in a mode that yielded a Fermi-level width of 0.4 eV for Ag metal and at a full width at half-maximum of 0.54 eV for Ag $3d_{5/2}$ core level peak. Energy scale was calibrated using the Fermi level of clean Ag. Phosphorescence spectra were measured in dichloromethane using an Edinburgh FPLS 920 fluorescence spectrophotometer at 77 K cooling by liquid nitrogen. The crystal suitable for X-ray single-crystal diffraction analysis was obtained through the slow evaporation of the ethanol solution of the compound at room temperature. All diffraction data were collected at 295 K on a RIGAKU RAXIS-RAPID diffractometer with graphite monochromatized Mo-$K\alpha$ (λ = 0.71073 Å) radiation in ω scan mode. All structures were solved by direct method and difference Fourier syntheses. Non-hydrogen atoms were refined by full-matrix least-squares techniques on F^2 with anisotropic thermal parameters. The hydrogen atoms attached to carbons were placed in calculated positions with C−H = 0.93 Å and U(H) = 1.2 U_{eq}(C) in the riding model approximation. All calculations were carried out with the SHELXL97 program.

Synthesis. *2′,7′-Dibromospiro[fluorene-9,9′-xanthene] (**4**).*[13] CH_3SO_3H (2.14 mL, 24.4 mmol) was added dropwise to a mixture of 2-bromo-9H-fluoren-9-one (5.92 g, 24.3 mmol) and phenol (5.04 g, 12.1 mmol) in a three neck flasks. This mixture was stirred under nitrogen for 2 h at 150 °C before being quenched with water. The sodium hydroxide aqueous solution (50%) was added in dropwise until pH of the mixture was adjusted to 7−8. The mixture was then extracted with dichloromethane (50 mL × 3). The combined extract was dried ($MgSO_4$) and then concentrated under reduced pressure. The residue

dx.doi.org/10.1021/cm201654c |*Chem. Mater.* 2011, 23, 5331–5339

was purified through column chromatography (SiO_2; petroleum ether) to yield 2 as a white solid (2.56 g, 71%); mp 249 °C.

^{1}H NMR (400 MHz, DMSO-d_6, δ): 8.02(d, 2H, J = 7.6 Hz), 7.434−7.491 (m, 4H), 7.321−7.281 (t, 4H, J = 8.8 Hz), 7.148 (d, 2H, J = 7.6 Hz), 6.265 (d, 2H, J = 2.4 Hz). ^{13}C NMR (75 MHz, DMSO-d_6, δ): 156.6, 151.1, 137.6, 131.4, 129.1, 128.7, 127.8, 123.6, 123.1, 122.4, 121.4, 117.1, 54.3. HRMS (m/z): 488 [M^+]. Elemental anal. Calcd (%) for $C_{25}H_{14}Br_2O$: C, 61.26; H, 2.88; O, 3.26. Found: C, 61.33; H, 2.91; O, 3.42.

Biphenyl(spiro[fluorene-9,9′-xanthen]-2-yl) Phosphine Oxide (SFX2PO). *n*-BuLi (1.6 M in hexane, 3.40 mL, 8.50 mmol) was added dropwise to a stirred solution of 2 (2.61 g, 4.07 mmol) in anhydrous THF (200 mL) under a nitrogen atmosphere at −78 °C. After the solution was stirred at −78 °C for an additional 3 h, chlorodiphenylphosphine (CDPP) (1.58 mL, 8.59 mmol) was added to provide a clear, pale-yellow solution. The mixture was warmed gradually to room temperature under stirring and further reacted overnight. The reaction was quenched through the addition of water (200 mL) and the mixture was then extracted with ethyl acetate (2 × 100 mL). The combined extract was dried ($MgSO_4$) and then concentrated under reduced pressure. The rude product was dissolved in dichloromethane (50 mL) and then 30% aqueous hydrogen peroxide (5 mL) was added. The mixture was stirred at room temperature for 3 h and then extracted with dichloromethane (3 × 50 mL). The collected organic phase was dried ($MgSO_4$) and then concentrated under reduced pressure. The residue was purified through column chromatography (SiO_2; ethyl acetate/methanol, 50:1) to yield SFX2PO as a white solid (2.56 g, 49%).

^{1}H NMR (400 MHz, DMSO-d_6, δ): 8.139 (t, 1H, J = 2.2,7.8 Hz), 8.06 (d, 1H, J = 7.6 Hz), 7.573−7.387 (m, 13H), 7.316 (t, 1H, J = 7.6 Hz), 7.251 (t, 4H, J = 8.0 Hz), 7.120 (d, 1H, J = 7.6 Hz), 6.834 (m, 2H), 6.282 (d, 2H, J = 7.6 Hz). ^{13}C NMR (75 MHz, DMSO-d_6, δ): 155.359, 154.972 (d, $J_{C,P}$ = 11.9 Hz), 151.160, 143.480, 138.373, 133.233, 133.115 (d, $J_{C,P}$ = 102.9 Hz), 132.539 (d, $J_{C,P}$ = 2.2 Hz), 132.263, 132.145, 131.850 (d, $J_{C,P}$ = 9.9 Hz), 129.857 (d, $J_{C,P}$ = 114.7 Hz), 128.957, 129.179 (d, $J_{C,P}$ = 11.9 Hz), 128.560 (d, $J_{C,P}$ = 9.1 Hz), 127.640, 125.827, 124.243, 124.144, 122.004, 121.354 (d, $J_{C,P}$ = 13.4 Hz), 117.380, 54.263. ^{31}P NMR (400 MHz, $CDCl_3$, δ): 29.2. HRMS (m/z): 532 [M^+]. Elemental anal. Calcd (%) for $C_{37}H_{25}O_2P$: C, 83.44; H, 4.73; O, 6.01. Found: C, 83.53; H, 4.76; O, 6.19.

Spiro[fluorene-9,9′-xanthene]-2,7-diylbis(biphenylphosphine oxide) (SFX27PO). The synthetic method was similar to that of SFX2PO. The residue was purified through column chromatography (SiO_2; petroleum ether/ethyl acetate/ethanol, 2:2:1) to yield SFX27PO as a white solid (2.02 g, 45%).

^{1}H NMR (400 MHz, DMSO-d_6, δ): 8.225 (dd, 2H, J = 2.4,7.9 Hz), 7.551−7.639 (m, 6H), 7.408−7.512 (m, 18H), 7.248−7.269 (m, 4H), 6.847−6.887 (m, 2H), 6.314 (d, 2H, J = 7.6 Hz). ^{13}C NMR (75 MHz, DMSO-d_6, δ): 155.231 (d, $J_{C,P}$ = 12.1 Hz), 151.159, 142.132, 133.772, 132.909 (d, $J_{C,P}$ = 102.9 Hz), 132.613 (d, $J_{C,P}$ = 2.6 Hz), 132.401 (d, $J_{C,P}$ = 11.2 Hz), 131.856 (d, $J_{C,P}$ = 9.8 Hz), 129.589, 129.210 (d, $J_{C,P}$ = 11.9 Hz), 128.938 (d, $J_{C,P}$ = 66.6 Hz), 127.418, 124.414, 123.463, 122.385 (d, $J_{C,P}$ = 12.3 Hz), 117.528, 54.511; ^{31}P NMR (400 MHz, $CDCl_3$, δ): 29.1. HRMS (ESI, m/z): 732[M + H]$^+$. Elemental anal. Calcd (%) for $C_{49}H_{34}O_3P_2$: C, 80.32; H, 4.68; O, 6.55. Found: C, 80.45; H, 4.74; O, 6.74.

Biphenyl (Spiro[fluorene-9,9′-xanthen]-2′-yl)phosphine oxide (SFX2′PO) and Spiro[fluorene-9,9′-xanthene]-2′,7′-diylbis(diphenylphosphine oxide) (SFX2′7′PO). The synthetic method used was similar to that of SFX2PO. The residue was purified through column chromatography (SiO_2; ethyl acetate/Petroleum ether, 1:1) to yield SFX2′PO as a white solid (0.7 g, 32%);

^{1}H NMR (400 MHz, DMSO-d_6, δ): 7.919 (d, 2H, J = 7.6 Hz), 7.519 (m, 2H), 7.438 (m, 1H), 7.41−7.36 (m, 7H), 7.34−7.28 (m, 7H), 7.23 (m, 2H), 7.09 (d, 2H, J = 7.6 Hz), 6.89−6.85 (m, 1H), 6.608 (m, 1H), 6.277 (m, 1H, J = 1.4,7.8 Hz). ^{13}C NMR (75 MHz, DMSO-d_6, δ): 154.445, 154.076 (d, $J_{C,P}$ = 2.9 Hz), 150.926, 139.544, 133.343 (d, $J_{C,P}$ =11.9 Hz), 132.887, 131.967 (d, $J_{C,P}$ =11.1 Hz), 132.365 (d, $J_{C,P}$ = 104.6 Hz), 131.812 (d, $J_{C,P}$ =9.8 Hz), 131.601 (d, $J_{C,P}$ =2.8 Hz), 128.326 (d, $J_{C,P}$ =5.5 Hz), 128.179, 128.006, 123.545 (d, $J_{C,P}$ =94.6 Hz), 126.002, 125.635 (d, $J_{C,P}$ =13.1 Hz), 125.397, 124.690, 123.955, 120.084, 117.203 (d, $J_{C,P}$ =13.1 Hz), 116.843, 53.928. ^{31}P NMR (400 MHz, $CDCl_3$, δ): 28.6. HRMS (m/z): 532 [M+]. Elemental anal. Calcd (%) for $C_{37}H_{25}O_2P$: C, 83.44; H, 4.73; O, 6.01. Found: C, 83.51; H, 4.79; O, 6.23.

Through column chromatography (SiO_2; ethyl acetate/petroleum ether, 2:1) to yield SFX2′7′PO as a white solid (0.4 g, 13%).

^{1}H NMR (400 MHz, DMSO-d_6, δ): 7.864 (d, 2H, J = 7.6), 7.54−7.47 (m, 6H), 7.413−7.351 (m, 12H), 7.324−7.277 (m, 8H), 7.229 (m, 2H), 7.13 (d, 2H, J = 7.55), 6.613 (m, 2H). ^{13}C NMR (75 MHz, DMSO-d_6, δ): 154.111, 153.392 (d, $J_{C,P}$ = 2.9 Hz), 139.374, 132.81 (d, $J_{C,P}$ = 103.23), 132.422 (d, $J_{C,P}$ = 2.6 Hz), 132.318, 132.262, 132.150, 131.623 (d, $J_{C,P}$ = 9.7 Hz), 129.309, 129.079 (d, $J_{C,P}$ = 11.9 Hz), 128.191 (d, $J_{C,P}$ = 105.3 Hz), 125.649, 125.508 (d, $J_{C,P}$ = 2.6 Hz), 121.137, 118.129 (d, $J_{C,P}$ = 12.7 Hz), 53.747. ^{31}P NMR (400 MHz, $CDCl_3$, δ): 28.5. HRMS (ESI, m/z): 732 [M + H]$^+$. Elemental anal. Calcd (%) for $C_{49}H_{34}O_3P_2$: C, 80.32; H, 4.68; O, 6.55. Found: C, 80.41; H, 4.76; O, 6.69.

Theoretical Calculations. Computations on the electronic ground state of the compounds were performed using Becke's three-parameter density functional in combination with the nonlocal correlation functional of Lee, Yang, and Parr (B3LYP).[16,17] 6-31G(d) basis sets were employed. The ground-state geometries were fully optimized at the B3LYP level. All computations were performed using the Gaussian 03 package.[18]

Device Fabrication. For device fabrication, all of the PO compounds were recrytallized for three to four times from their CH_2Cl_2/ethyl acetate solutions until their purification excess 99% determined with High Performance Liquid Chromatography (HPLC) (99.3% for SFX2PO, 99.2% for SFX27PO, 99.4% for SFX2′PO and 99.1% for SFX2′7′PO). All the devices were fabricated onto prepatterned indium−tin oxide (ITO) with a sheet resistance of 10 Ω/square. The substrates were ultrasonic cleaned sequentially with detergent, acetone, ethanol, and deionized water, then dried in an oven, and finally treated in an ultraviolet-ozone chamber. After the organic deposition, 100-nm-thick Al was covered directly on the organic layers serving as cathode. The cathode area defines an active device area of 2 × 2 mm^2 through a shadow mask. Current−voltage-luminance (J−V−L) characteristics were measured with a PR650 spectrascan spectrometer and a Keithley 2400 programmable voltage−current source. EQE was determined with the method mentioned in the literature.[19] All the measurements were carried out in the ambient environment without encapsulation.

RESULTS AND DISCUSSION

Synthesis and Morphological Stability. The spiro-PO compounds were conveniently prepared through a three-step procedure of lithiation, phosphorization and oxidation with moderate yields (Scheme 2). The structural characterization was established on the basis of highly resolved mass spectrometry and NMR spectroscopy (see the Supporting Information). The molecular structures were further confirmed by X-ray Crystallography (Figure 1). It indicated that the adjacent molecules of SFX27PO were bridged by water molecules through the P−H···O hydrogen-bonding interactions to generate a 1D chain structure along *c* axis (Figure 1a). For SFX2′PO, two types intermolecular C−H···π interactions (3.585 and 3.668 Å) were observed (Figure 1b), which connected adjacent molecules into a 1D chain structure along *a* axis. But for SFX2′7′PO, the asymmetric unit cell

Scheme 2[a]

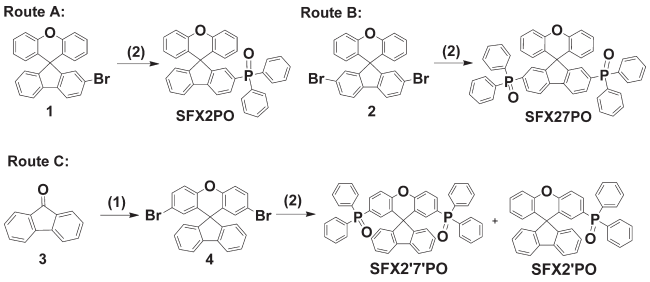

[a] Reaction condition: (1) 4-bromophenol, $MeSO_3H$, 150 °C, 48 h; (2) a) n-BuLi,-78 °C,2h, b) CDPP, −78 °C, 24h, (d) CH_2Cl_2, H_2O_2.

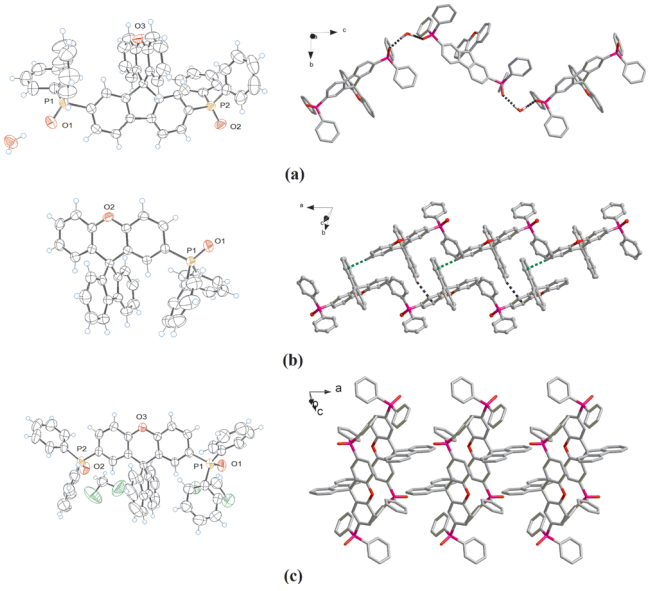

Figure 1. Single-crystal structures and packing diagrams of (a) SFX27PO, (b) SFX2′PO, and (c) SFX2′7′PO.

comprised of SFX2′7′PO and two solvent dichloromethane molecules as shown in Figure 1c, and no aromatic $\pi-\pi$ stacking interactions were detected between adjacent molecules. It indicated that these PO compounds have very weak intermolecular interaction, which is advantageous to restrain the nonradiative energy loss attributed to the multiparticle quenching effects.[14] The thermal and morphological stability of the spiro-PO hosts were also investigated by the thermogravimetric analysis (TGA) and the differential scanning calorimetry (DSC) (Table 1 and Figure SI19 in the Supporting Information). Although no distinct temperature of glass-transition (T_g) was observed, the melting points (T_m) of the spiro-PO compounds are improved remarkably compared with SFX (∼50 °C for SFX2PO and SFX2′PO, and ∼100 °C for SFX27PO and SFX2′7′PO). Simultaneously, their temperatures of decomposition (T_d) are also greatly higher than that of SFX with the increases of ∼90 °C for SFX2PO and SFX2′PO, and ∼170 °C for SFX27PO and SFX2′7′PO, which facilitates the device fabrication through vacuum evaporation. Moreover, T_d and T_m of SFX2PO and SFX27PO are higher than those of SFX2′PO and SFX2′7′PO. The better thermal performance makes SFX2PO and SFX27PO advantageous in the film morphology stability and suppresses the

Table 1. Physical Properties of the PO Hosts

compd	Abs (nm)	FL (nm)	T_1 (eV)	T_d (°C)
SFX	306, 263, 232[a]	311, 321[a]	2.87	258
	308, 296, 264[b]	340[b]		
SFX2PO	312, 283, 230[a]	321, 333[a]	2.78	379
	312, 290[b]	364[b]		
SFX27PO	319, 291, 227[a]	385[a]	2.70	466
	322, 293[b]	380[b]		
SFX2′PO	304, 263, 229[a]	311, 321[a]	2.86	368
	307, 282[b]	328[b]		
SFX2′7′PO	304, 269, 229[a]	311, 321[a]	2.83	462
	307, 282[b]	325[b]		

[a] In CH_2Cl_2 (1×10 −6 mol L-1); [b] In film.

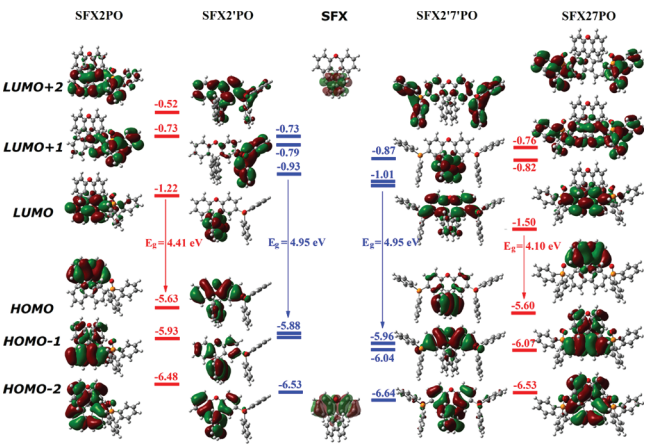

Figure 2. DFT calculation results of the spiro-PO compounds.

potential of phase separation during device operating compared with their 2′,7′-position substituted counterparts.

Simulation Results. The effect of the substitution position on FMOs of the spiro-PO compounds was investigated with the density functional theory (DFT) calculations (Figure 2 and Table SI1 in the Supporting Information). For SFX2PO and SFX27PO, their HOMO and LUMO were mainly contributed by xanthene and fluorene moieties, respectively. It is believed that the separated FMOs can facilitate the balanced carrier injecting/transporting.[15] However, for SFX2′PO, although xanthene is substituted with DPPO group, its LUMO is located at fluorene while its HOMO is contributed by both xanthene and fluorene. This implies that the electron-injecting ability of fluorene is stronger than that of xanthene while the hole injecting ability of xanthene is equivalent to that of fluorene even if the electron-withdrawing DPPO is introduced at xanthene. Therefore, for SFX2′PO, the polarizing effect of DPPO is actually misemployed, since DPPO has no contribution to the electron injection of SFX2′PO but reduces its HOMO. This abandons the advantage of P═O moieties as the carrier-transporting type insulating group. Substituted with two DPPOs, FMOs of SFX2′7′PO are separated, as the HOMO is located at fluorene while the LUMO is located at xanthene. It indicates that the stronger withdrawing effect of more DPPOs makes the substituted xanthene obtain the stronger electron injecting ability and weaker hole injecting ability than fluorene. Actually, compared with SFX2′PO, the enhanced electron injecting ability of SFX2′7′PO is accompanied

dx.doi.org/10.1021/cm201654c |Chem. Mater. 2011, 23, 5331–5339

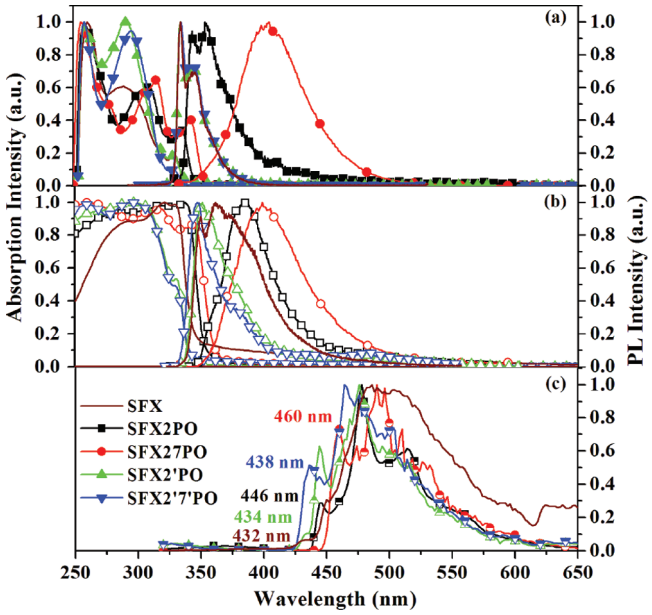

Figure 3. Absorption and emission (FL) spectra of the spiro-PO compounds (a) in CH_2Cl_2 (1×10^{-6} M) and (b) in film, and (c) PH spectra of the spiro-PO compounds in CH_2Cl_2 (1×10^{-6} M) at 77 K.

with its reduced hole-injecting ability, which is also proved by the same energy gaps of SFX2′PO and SFX2′7′PO and the same differences between their FMOs. This result is in accord with the DPPO substituted carbazole hosts (see Figure SI20 in the Supporting Information).[10a] Because in SFX2PO and SFX27PO DPPOs are introduced at more electrophilic fluorene, the improved effect of DPPOs on the electron injection is further amplified. LUMOs of SFX2PO and SFX27PO are significantly lower than those of SFX2′PO and SFX2′7′PO. This difference is bigger when more DPPO moieties are introduced (0.3 eV for SFX2PO and SFX2′PO and 0.5 eV for SFX27PO and SFX2′7′PO). More significantly, different with their 2′,7′-position substituted counterparts, HOMO of SFX27PO is equivalent with that of SFX2PO while more DPPOs make LUMO of the former for 0.3 eV lower than that of the latter. Therefore, the electron-withdrawing effect of DPPOs is used to improve the electron injection in the spiro-PO compounds without reducing their hole injecting ability through the reasonable choice of substitution at the electrophilic fluorene. He I Ultraviolet Photoelectron Spectroscopy (UPS) spectra of the spin-coated films of SFX2PO, SFX27PO, SFX2′PO and SFX2′7′PO were measured to determine their ionization potentials (see Figure SI21 in the Supporting Information), which are 5.43, 5.28, 6.35, and 6.31 (±0.05) eV, respectively. It is exactly in accord with the results of Gaussian calculation.

Optical Properties. UV/vis and photoluminescent (PL) spectra of the spiro-PO compounds and SFX in dilute CH_2Cl_2 solutions (1×10^{-6} mol L^{-1}) and in film were measured to investigate their optical properties (Figure 3). In solution, SFX has three absorption bands at 306, 262, and 232 nm, respectively. The weakest band at 306 nm is attributed to n→π^* transition from xanthene to fluorene, which becomes weaker in the spectra of SFX2′PO and SFX2′7′PO due to the electron-withdrawing effect of DPPOs on xanthene. This band remarkably shifts bathochromicly by 6 nm for SFX2PO and 13 nm for SFX27PO, corresponding to 0.08 and 0.17 eV, respectively, which is ascribed to the depression of π^* orbital of their fluorene moieties. This is

Scheme 3. Structures of the Materials in the Devices and the Energy Level Diagram

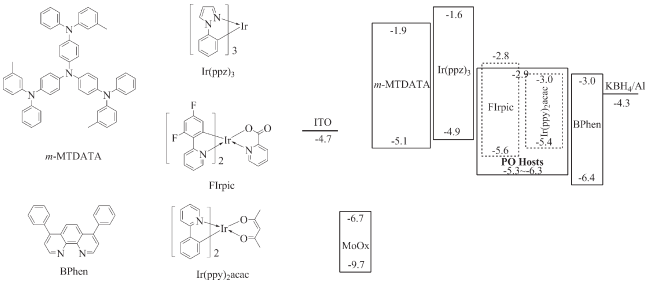

in accord with the results obtained from TDDFT calculation (see Figure SI22 in the Supporting Information). The stronger band of SFX at 262 nm is originated from the combination of n→π^* transition of xanthene and π→π^* transition of fluorene. For SFX2PO and SFX27PO, this band is divided into two kinds of bands as shoulder peaks around 249 nm from xanthene and the other peaks around 285 nm from fluorene, which are also attributed to DPPO substitution. The absorption bands around 230 nm in all of the absorption spectra are originated from π→π^* transition of xanthene. The singlet energy gaps of SFX2′PO and SFX2′7′PO are equivalent with that of SFX as 3.94 eV, whereas those of SFX2PO and SFX27PO are reduced to 3.85 and 3.74 eV, respectively. This trend is in accord with the calculation results (see Table S1 in the Supporting Information). PL spectra of SFX2′PO and SFX2′7′PO in solution are nearly the same with that of SFX, which implies the slight influence of 2′,7′-position substitution on the singlet excited state properties of the chromosphore core SFX. However, the emission peaks of SFX2PO and SFX27PO are at 321 and 380 nm with the bathochromic shifts of 10 and 70 nm (0.124 and 0.766 eV), respectively, for the same reason mentioned above. In film, the emission of SFX remarkably shifts red and becomes broader because of its worse aggregation in the solid state. It is shown that the spectra of the spiro-PO hosts exhibit reduced bathochromic shifts and the emissions of the disubstituted derivatives are more stable than those of the monosubstituted derivatives, because the strong steric effect of DPPOs restrains the intermolecular interaction. T_1 of these spiro-PO compounds were estimated from the $\upsilon_{0,0}$ transition identified as the highest-energy bands in their time-resolved PH spectra at 77 K, which are 2.78, 2.70, 2.86, and 2.83 eV for SFX2PO, SFX27PO, SFX2′PO, and SFX2′7′PO, respectively. Compared with 2.87 eV of SFX, T_1 of these spiro-PO compounds are slightly reduced. It indicates that the 2,7-position substitution affects the excited levels of the chromophore more remarkably than the 2′,7′-position substitution. Nevertheless, compared with that of SFX, T_1 of SFX2PO is only reduced by less than 0.1 eV, which facilitates the exothermal energy transfer to the blue-emitting phosphor, such as iridium(III)bis-(4,6-(difluorophenyl)pyridinato-N,C2)picolinate (FIrpic, $T_1 \approx$ 2.65 eV).

DFT calculations and optophysical investigations reflected that although the 2,7-position substituted derivatives are superior in carrier injection with much more suitable FMOs, they show somewhat inferior in maintaining the excited energy levels of the chromophore. Based on these spiro-PO hosts, the question arises whether it is worth achieving better electrical properties with the cost of reduced T_1. We investigated it through the utilization of these hosts in blue- and green-emitting PHOLEDs.

dx.doi.org/10.1021/cm201654c |*Chem. Mater.* 2011, 23, 5331–5339

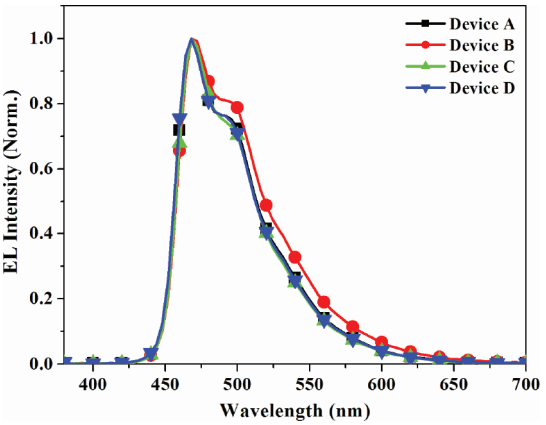

Figure 4. EL spectra of blue-emitting device A−D.

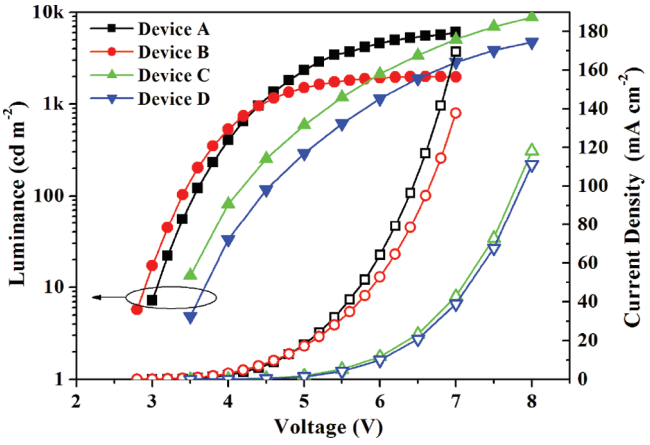

Figure 5. Brightness (solid)−current density (hollow) (J)−voltage (V) curves of blue-emitting devices A−D.

Electroluminescent Performance of Blue and Green PHOLEDs. The blue-emitting devices A-D based on SFX2PO, SFX27PO, SFX2′7′PO, and SFX2′7′PO, respectively, were fabricated with the configuration of ITO/MoO_x (2 nm)/4,4′,4″-tri(*N*-3-methylphenyl-*N*-phenylamino) triphenylamine (m-MTDATA):MoO_x (15 wt %, 30 nm)/*m*-MTDATA (10 nm)/Tris(phenylpyrazole)iridium ($Ir(ppz)_3$) (10 nm)/spiro-PO host: FIrpic (10 wt %, 10 nm)/ 4,7-diphenyl-1,10-phenanthroline (BPhen) (40 nm)/KBH_4 (1 nm)/Al were fabricated (Scheme 3), where MoO_x and KBH_4 served as hole- and electron-injecting layers, *m*-MTDATA and BPhen served as hole- and electron-transporting layers (HTL and ETL), $Ir(ppz)_3$ was used as hole-transporting and electron-blocking material, respectively. All of these devices exhibited stable blue emissions attributed to FIrpic (Figure 4).

The turn-on voltages of 2.8 and 3.0 V of devices A and B, respectively, were remarkably lower than the 3.5 V of devices C and D (Figure 5 and Table 2). Along with the increase in luminance, the difference in operating voltages between A, B and C, D was also increased (beyond 1.0 V at 1000 cd m^{-2}). It is noticed that the low driving voltage of 4.4 V of A and B at 1000 cd m^{-2} makes the application of these devices in portable equipment feasible. Obviously, this remarkable difference is originated from the much stronger carrier injecting/transporting ability of SFX2PO and SFX27PO than that of SFX2′PO and SFX2′7′PO,

Table 2. EL Performance of Devices A−H

device	driving voltage (V)[a]	maximum efficiency[b]	efficiency roll-off (%)[b]
A	3.0, 3.5, 4.4	19.8, 17.6, 10.1	19.7, 35.2, 18.8[c]
B	2.8, 3.4, 4.4	19.7, 18.2, 9.3	32.5,48.9, 32.3[c]
C	3.5, 4.1, 5.4	17.1, 17.2, 8.8	30.4, 54.1, 29.5[c]
D	3.5, 4.4, 5.9	8.7, 6.9, 4.5	26.4, 44.9, 33.3[c]
E	2.8, 3.2, 3.7	45.8, 41.1, 12.5	0.4, 5.1, 1.6[c]
			10.7, 29.4, 10.4[d]
F	2.4, 2.7, 3.3	70.0, 77.0, 19.1	2.3, 14.2, 2.1[c]
			16.9, 40.4, 16.2[d]
G	3.0, 3.5, 4.3	27.4, 21.5, 7.6	6.2, 14.9, 6.6[c]
			28.8, 49.8, 28.9[d]
H	3.2, 3.7, 4.4	27.3, 22.7, 7.5	7.7, 19.4, 8.0[c]
			22.7, 44.5, 22.7[d]

[a] In the turn of turn-on, at 100 cd m^{-2} and at 1000 cd m^{-2}; [b] In the turn of C.E. (cd A^{-1}), P.E. (lm W^{1-}) and EQE (%); [c] At 1000 cd m^{-2}; [d] At 5000 cd m^{-2}.

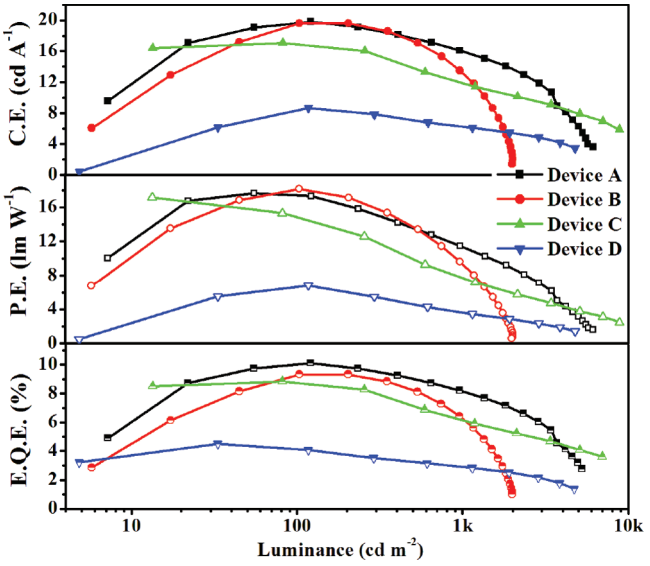

Figure 6. Efficiency curves of blue-emitting devices A−D.

which was also proved by the much higher current density (J) of A and B than that of C and D at the same driving voltages, respectively. At the voltage less than 4.0 V, the luminance of B was the highest among these four devices, which corresponded to the superior carrier injecting ability of SFX27PO among the spiro-PO hosts and demonstrated the significance of excellent carrier injecting in affecting the exciton recombination in EMLs. However, the luminance of B at voltages beyond 4.5 V did not further increase, which is supposed to be attributed to two factors: one is the notorious exciton quenching at high exciton concentrations due to the lower T_1 of SFX27PO with the poorer ability of high energy triplet confinement and its inferior stability under high electrical stress; the other is the remarkably dominant electron injecting/transporting ability of SFX27PO, which may give rise to the mismatched carrier injecting/transporting of SFX27PO and FIrpic. The latter seems more important since it can induce triplet excitons diffused from the EML host into other layers and lost to nonradiative decay pathways.[20]

dx.doi.org/10.1021/cm201654c |*Chem. Mater.* 2011, 23, 5331–5339

Nevertheless, at the luminance below 1000 cd m^{-2} the efficiencies of B were still higher than those of C and D (Figure 6). With the higher T_1 and relatively balanced carrier-injecting ability, SFX2PO endowed Device A with the highest efficiencies among these four devices including maximum current efficiency (C.E.) of 19.8 cd A^{-1}, power efficiency (P.E.) of 17.6 lm W^{-1} and external quantum efficiency (E.Q.E.) of 10.1%. Although SFX2′PO and SFX2′7′PO have higher T_1 than SFX2PO, the maximum efficiencies of devices C and D were lower than those of A, and these two devices showed more remarkable efficiency roll-off. Due to the same reasons mentioned above, the efficiencies of C became higher than those of A at very high brightness. Simultaneously, device D exhibited the worst EL performance among these four devices with the highest driving voltage and the lowest efficiencies at a required luminance level for display and indoor lighting, which is attributed to the worst carrier injecting/transporting ability of SFX2′7′PO among these spiro-PO hosts, even though T_1 of its host SFX2′7′PO is higher than that of SFX2PO. This is in accordance with the empirical regularity of higher T_1 usually corresponding to worse carrier injecting/transporting ability. Furthermore, weak triplet excition confinement in the EML/electron transporting layer (ETL) interface in our structures may also play a role. The carrier transporting characteristics of the PO hosts were investigated through their nominal hole-only and electron-only devices with the configurations of ITO/MoO_x (2 nm)/m-MTDATA (10 nm)/ $Ir(ppz)_3$ (10 nm)/PO Host (60 nm)/$Ir(ppz)_3$ (10 nm)/m-MTDATA (10 nm)/MoO_x (2 nm)/Al (hole-only) and ITO/KBH4 (1 nm)/BPhen (20 nm)/PO Host (60 nm)/BPhen (20 nm)/KBH4 (1 nm)/Al (electron-only) (see Figure SI25 in the Supporting Information). It indicated that the hole transporting abilities of SFX2PO and SFX27PO are stronger than those of their 2′,7′-substituted counterparts, which demonstrated that the substitution of DPPOs on relatively electron-insufficient moieties is beneficial to maintain the hole transporting properties of the chromophore core. This is further proved by the similar hole transporting characteristics of SFX2PO and SFX27PO. However, compared with SFX2′PO, the hole transporting ability of SFX2′7′PO was remarkably reduced for about 20 times, which should be ascribed to the immoderate substitution on electron-rich xanthene moiety. Simultaneously, the electron transporting abilities of SFX2PO and SFX2′PO are similar, but weaker than that of SFX27PO and stronger than that of SFX2′7′PO. Consequently, among these PO hosts, SFX27PO has the strongest carrier transporting ability and SFX2′7′PO the worst, which is in accordance with their carrier injecting ability. Therefore, it can be concluded that even for the blue-emitting PHOLEDs, the balanced carrier injecting/transporting still serves as the main factor in determining the driving voltage and the rates of exciton formation and concomitant radiative recombination. For an efficient and low-driving voltage PHOLEDs, a suitable host should possess both balanced carrier injecting/transporting ability and suitable T_1.

Usually, the hosts with too high triplet level and subsequently huge host−guest triplet level difference may suffer from an energy loss in host−guest energy transfer. Interestingly, our spiro-PO matrices also serve as excellent hosts for green phosphors.[8] The results (shown in Figures 7 and 8) were achieved from the green-emitting devices E-H based on SFX2PO, SFX27PO, SFX2′PO and SFX2′7′PO, respectively, whose structures were similar with those of the blue-emitting devices except for the different dopant as iridium(III)bis(2-phenylpyridinato-C2,N)acetylacetonate

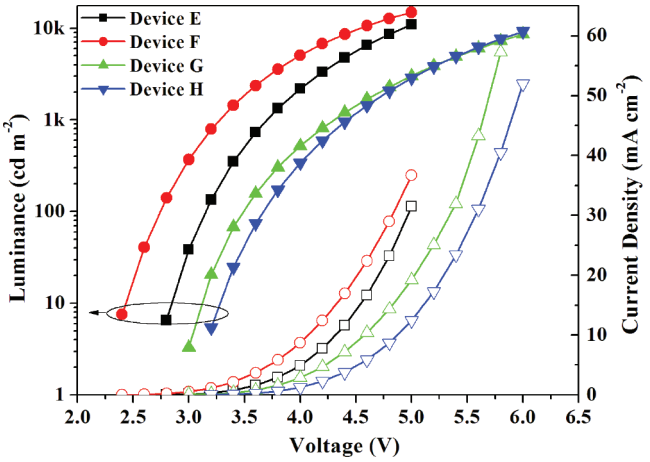

Figure 7. Brightness (solid)−current density (hollow) (J)−voltage curves of green-emitting devices E−H.

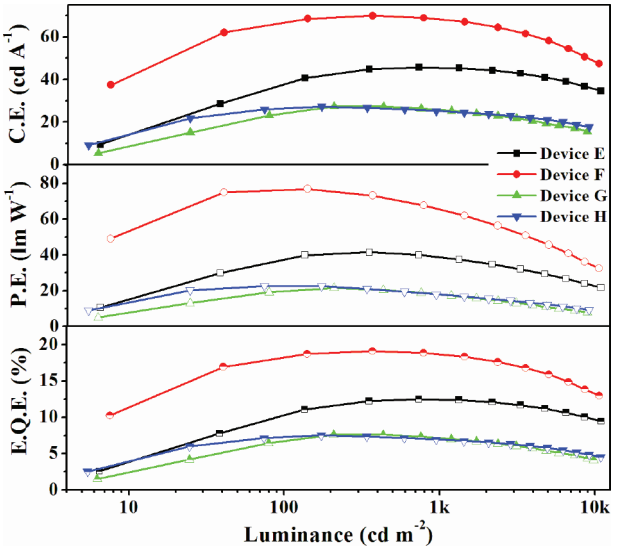

Figure 8. Efficiency curves of green-emitting devices E−H.

($Ir(ppy)_2acac$) and its different concentration of 6%. Both Device E and F exhibited extremely low operating voltages less than 4 V at 1000 cd m^{-2} (Figure 7). The driving voltages of Device F were still the lowest among these devices due to the best carrier injecting ability of SFX27PO host. Furthermore, the driving voltages of device F−H were also in accord with the carrier injecting ability of the corresponding spiro-PO hosts. T_1 of $Ir(ppy)_2acac$ is only 2.4 eV, which makes the exothermal energy transfer from all spiro-PO hosts to the guest feasible. This roughly allows the deviation of T_1 of the hosts to be less considerable. Therefore, the carrier injecting/transporting in EMLs directly influenced EL performance of these devices. It is shown that based on SFX27PO with the strongest carrier injecting ability Device F had the impressively high maximum efficiencies of 70.0 cd A^{-1}, 77.0 lm W^{-1} and 19.2% (Figure 8), which were the highest among these four green-emitting devices. Device E also realized moderate efficiencies exceeding 45 cd A^{-1}, 40 lm W^{-1}, and 10%, respectively. Contrarily, both devices G and H exhibited much lower efficiencies, which were nearly one-third that of device F. It was showed that the efficiency roll-offs of these

dx.doi.org/10.1021/cm201654c |Chem. Mater. 2011, 23, 5331–5339

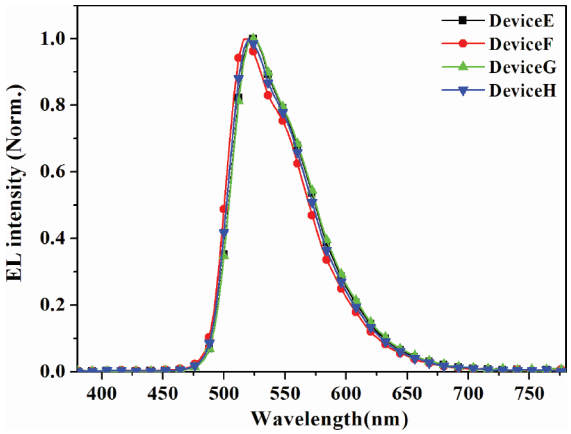

Figure 9. EL spectra of green-emitting devices E−H.

green devices were dramatically reduced, compared with that of the blue devices. The high and stable efficiencies of E and F should be profited from the matched carrier injecting/transporting ability of their hosts and $Ir(ppy)_2acac$. The EL spectra of all of these green devices were originated from $Ir(ppy)_2acac$ and stable during voltage increasing (Figure 9).

The results of the blue and green-emitting PHOLEDs reflected that the excellent carrier injecting/transporting ability of the hosts is one of the main factors directly affecting EL performance, including the driving voltage and efficiencies. In low exciton concentration, the efficient and balanced carrier injection and transporting in EMLs play an effective role in maintaining high EL efficiency and a host with too high triplet level would induce energy loss due to the nonradiative relaxation and host−guest interaction. This indicates that it is not advisible to achieve too high T_1 and facilitate electron injection through PO moieties with the cost of weakening the hole injection ability of the chromophores. The ideal strategy is preserving high enough T_1 and improving electron injection by utilizing PO moieties without reducing hole injection in the hosts. However, it is still greatly challenging to achieve satisfied ambipolar host for high T_1 guests. Although not perfect, SFX2PO and SFX27PO already pave one way for the highly efficient low-voltage PHOLEDs.

CONCLUSION

In summary, four DPPO substituted SFX derivatives, SFX2PO, SFX27PO, SFX2′PO, and SFX2′7′PO, were designed and synthesized to investigate the influence of substitution position on their chemical and optophysical properties. The improved morphological and thermal stability was proved by single-crystal diffraction and thermal analysis. It indicates that DPPOs substituted on relatively electron-rich xanthene reduce both LUMO and HOMO, while remaining HOMO and reducing LUMO can be simultaneously realized through substituting DPPOs on relatively electron-deficient fluorene. Therefore, the introduction of electron-withdrawing DPPOs in electron-deficient moieties in the molecules accompanied with suitable linkages insulating the electron-rich and deficient moieties can endow the hosts with much better carrier injecting ability and high enough T_1 for blue and green phosphors. The optophysical investigation showed that the 2,7-position substitution affects the excited levels of the chromophore more than the 2′,7′-position substitution. Nevertheless, compared with that of SFX, T_1 of SFX2PO is reduced only by less than 0.1 eV and comparable with those of SFX2′PO and SFX2′7′PO. On the basis of the blue- and green-emitting PHOLEDs, the influences of the carrier injecting/transporting ability in EMLs and high T_1 on EL performances were investigated. It is shown that the carrier injecting/transporting ability of the hosts directly determined both $I-V$ characteristics and the efficiencies. Furthermore, at a practical luminance (such as 1000 cd m^{-2}), the carrier injecting/transporting in EMLs was predominant over high T_1 to ensure the efficient exciton formation and radiative decay. Under very high luminance, host−guest energy loss and the complicated annihilation process should be well-managed to reduce the efficiency roll-offs. Therefore, for the efficient and low-voltage devices, in case T_1 of the hosts were higher than those of the phosphors, the carrier injecting/transporting behaviors in EMLs seems more important than extremely high T_1, as a suitable host−guest system will satisfy a resonant triplet energy transfer from the host to the guest with nearly no energy loss. It is shown that the amplified discrepancy of the moieties with different electrical properties indeed influences the excited energy levels. To solve this problem, either chromophores with suitable T_1 or more effective insulating linkages should be involved in. The relevant work is ongoing in our laboratory.

ASSOCIATED CONTENT

Supporting Information. NMR spectra, Gaussian simulation results of the PO-substituted carbazole derivatives, TGA curves, XPS spectra, efficiencies−J curves of devices A−H and $J-V$ curves of single-carrier devices. This material is available free of charge via the Internet at http://pubs.acs.org.

AUTHOR INFORMATION

Corresponding Author

*Fax: (+86) 451-86608042 (H.X.). E-mail: hxu@hlju.edu.cn (H.X.); wei-huang@njupt.edu.cn (W.H.); zhao_yi@jlu.edu.cn (Y.Z.).

Author Contributions

‡J.Z. and G.X. have made equal contributions to this work.

ACKNOWLEDGMENT

For the financial support, we thank the "973" project (2009CB930600 and 2010CB327701), NSFC (Grants 50903028, 20972043, 20704023, 60876010, 60706017, 60977024, 20774043, 61176020, and 60907047), the Key Project of Chinese Ministry of Education (104246, 208050, 707032), Natural Science Foundation of Jiangsu Province (Grants BK2009423, BK2008053, 08KJB510013, BK2008053, SJ209003, and TJ209035), Open Funds of KLOEID, Supporting Project of New Century Talents of Heilongjiang Province, Education Bureau of Heilongjiang Province (10td03) and Heilongjiang University (2010td08).

REFERENCES

(1) Baldo, M. A.; O'Brien, D. F.; You, Y.; Shoustikov, A.; Sibley, S.; Thompson, M. E.; Forrest, S. R. *Nature* **1998**, *395*, 151–154.

(2) (a) Baldo, M. A.; Lamansky, S.; Burrows, P. E.; Thompson, M. E.; Forrest, S. R. *Appl. Phys. Lett.* **1999**, *75*, 4–6. (b) Reineke, S.; Walzer, K.; Leo, K. *Phys. Rev. B* **2007**, *75*, 125328. (c) Song, D.; Zhao, S.; Luo, Y.; Aziz, H. *Appl. Phys. Lett.* **2010**, *97*, 243304.

(3) Kamtekar, K. T.; Monkman, A. P.; Bryce, M. R. *Adv. Mater.* **2010**, *22*, 572–584.

(4) Adachi, C.; Kwong, R. C.; Djurovich, P.; Adamovich, V.; Baldo, M. A.; Thompson, M. E.; Forrest, S. R. *Appl. Phys. Lett.* **2001**, *79*, 2082–2084.

(5) (a) Holmes, R. J.; Forrest, S. R.; Tung, Y.-J.; Kwong, R. C.; Brown, J. J.; Garon, S.; Thompson, M. E. *Appl. Phys. Lett.* **2003**, *82*, 2422–2424. (b) Tokito, S.; Iijima, T.; Suzuri, Y.; Kita, H.; Tsuzuki, T.; Sato, F. *Appl. Phys. Lett.* **2003**, *83*, 569–571.

(6) Ye, S. H.; Liu, Y. Q.; Di, C. A.; Xi, H. X.; Wu, W. P.; Wen, Y. G.; Lu, K.; Du, C. Y.; Liu, Y.; Yu, G. *Chem. Mater.* **2009**, *21*, 1333–1342.

(7) (a) Vecchi, P. A.; Padmaperuma, A. B.; Qiao, H.; Sapochak, L. S.; Burrows, P. E. *Org. Lett.* **2006**, *8*, 4211–4214. (b) Sapochak, L. S.; Padmaperuma, A. B.; Vecchi, P. A.; Qiao, H.; Burrows, P. E. *Proc. SPIE* **2006**, *6333*, 63330F.

(8) (a) Holmes, R. J.; D'Andrade, B. W.; Forrest, S. R.; Ren, X.; Li, J.; Thompson, M. E. *Appl. Phys. Lett.* **2003**, *83*, 3818–3820. (b) Ren, X.; Li, J.; Holmes, R. J.; Djurovich, P. I.; Forrest, S. R.; Thompson, M. E. *Chem. Mater.* **2004**, *16*, 4743–4747.

(9) (a) Padmaperuma, A. B.; Sapochak, L. S.; Burrows, P. E. *Chem. Mater.* **2006**, *18*, 2389–2396. (b) Cai, X.; Padmaperuma, A. B.; Sapochak, L. S.; Vecchi, P. A.; Burrows, P. E. *Appl. Phys. Lett.* **2008**, *92*, 083308. (c) Sapochak, L. S.; Padmaperuma, A. B.; Cai, X.; Male, J. L.; Burrows, P. E. *J. Phys. Chem. C* **2008**, *112*, 7989–7996. (d) Bhansali, U. S.; Polikarpov, E.; Swensen, J. S.; Chen, W.-H.; Jia, H.; Gaspar, D. J.; Gnade, B. E.; Padmaperuma, A. B.; Omary, M. A. *Appl. Phys. Lett.* **2009**, *95*, 233304. (e) Hsu, F.-M.; Chien, C.-H.; Shu, C.-F.; Lai, C.-H.; Hsieh, C.-C.; Wang, K.-W.; Chou, P.-T. *Adv. Funct. Mater.* **2009**, *19*, 2834–2843. (f) Polikarpov, E.; Swensen, J. S.; Chopra, N.; So, F.; Padmaperuma, A. B. *Appl. Phys. Lett.* **2009**, *94*, 223304. (g) Han, C.; Xie, G.; Xu, H.; Zhang, Z.; Yu, D.; Zhao, Y.; Yan, P.; Deng, Z.; Liu, S. *Chem.—Eur. J.* **2011**, *17*, 445–449. (h) Han, C.; Xie, G.; Xu, H.; Zhang, Z.; Xie, L.; Zhao, Y.; Liu, S.; Huang, W. *Adv. Mater.* **2011**, *23*, 2491–2496. (i) Jang, S. E.; Joo, C. W.; Jeon, S. O.; Yook, K. S.; Lee, J. Y. *Org. Electron.* **2010**, *11*, 1059–1065. (j) Son, H. S.; Seo, C. W.; Lee, J. Y. *J. Mater. Chem.* **2011**, *21*, 5638–5644. (k) Son, H. S.; Lee, J. Y. *Org. Electron.* **2011**, *12*, 1025–1032. (l) Kim, D.; Salman, S.; Veaceslav, C.; Salomon, E.; Padmaperuma, A. B.; Sapochak, L. S.; Kahn, A.; Brédas, J.-L. *Chem. Mater.* **2010**, *22*, 247–254.

(10) (a) Jeon, S. O.; Yook, K. S.; Joo, C. W.; Lee, J. Y. *Adv. Funct. Mater* **2009**, *19*, 3644–3649. (b) Jeon, S. O.; Yook, K. S.; Joo, C. W.; Lee, J. Y. *Adv. Mater.* **2010**, *22*, 1–5. (c) Jeon, S. O.; Jang, S. E.; Son, H. S.; Lee, J. Y. *Adv. Mater.* **2011**, *23*, 1436–1441.

(11) Chou, H.-H.; Cheng, C.-H. *Adv. Mater.* **2010**, *22*, 2468–2471.

(12) Yu, D.; Zhao, Y.; Xu, H.; Han, C.; Ma, D.; Deng, Z.; Gao, S.; Yan, P. *Chem.—Eur. J.* **2011**, *17*, 2592–2596.

(13) Xie, L.-H.; Liu, F.; Tang, C.; Hou, X.-Y.; Hua, Y.-R.; Fan, Q.-L.; Huang, W. *Org. Lett.* **2006**, *8*, 2787–2790.

(14) (a) Baldo, M. A.; Adachi, C.; Forrest, S. R. *Phys. Rev. B* **2000**, *62*, 10967–10977. (b) Giebink, N. C.; Forrest, S. R. *Phys. Rev. B* **2008**, *77*, 235215. (c) Reineke, S.; Walzer, K.; Leo, K. *Phys. Rev. B* **2007**, *75*, 125328.

(15) Tao, Y. T.; Wang, Q.; Yang, C. L.; Wang, Q.; Zhang, Z. Q.; Zou, T. T.; Qin, J. G.; Ma, D. G. *Angew. Chem.* **2008**, *120*, 8224–8227. *Angew. Chem., Int. Ed.* **2008**, *47*, 8104–8107.

(16) Becke, A. D. *J. Chem. Phys.* **1993**, *98*, 5648–5652.

(17) Lee, B.; Yang, W.; Parr, R. G. *Phys. Rev. B* **1988**, *37*, 785–789.

(18) Frisch, M. J.; Trucks, G. W.; Schlegel, H. B.; Scuseria, G. E.; Robb, M. A.; Cheeseman, J. R.; Montgomery, J. A. Jr.; Vreyen, T.; Kudin, K. N.; Burant, J. C.; Millam, J. M.; Iyengar, S. S.; Tomasi, J.; Barone, V.; Mennucci, B.; Cossi, M.; Scalmani, G.; Rega, N.; Petersson, G. A.; Nakatsuji, H.; Hada, M.; Ehara, M.; Toyota, K.; Fukuda, R.; Hasegawa, J.; Ishida, M.; Nakajima, T.; Honda, Y.; Kitao, O.; Nakai, H.; Klene, M.; Li, X.; Knox, J. E.; Hratchian, H. P.; Cross, J. B.; Adamo, C.; Jaramillo, J.; Gomperts, R.; Stratmann, R. E.; Yazyev, O.; Austin, A. J.; Cammi, R.; Pomelli, C.; Octhterski, J. W.; Ayala, P. Y.; Morokuma, K.; Voth, G. A.; Salvador, P.; Dannenberg, J. J.; Zakrzewski, V. G.; Dapprich, S.; Daniels, A. D.; Strain, M. C.; Farkas, O.; Malick, D. K.; Rabuck, A. D.; Raghavachari, K.; Foresman, J. B.; Ortiz, J. V.; Cui, Q.; Baboul, A. G.; Clifford, S.; Cioslowski, J.; Stefanov, B. B.; Liu, G.; Liashenko, A.; Piskorz, P.; Komaromi, I.; Martin, R. L.; Fox, D. J.; Keith, T.; Al-Laham, M. A.; Peng, C. Y.; Nanayakkara, A.; Challacombe, M.; Gill, P. M. W.; Johnson, B.; Chen, W.; Wong, M. W.; Gonzalez, C.; Pople, J. A. *Gaussian 03, Revision D.02*; Gaussian, Inc.: Pittsburgh, PA, 2004.

(19) Meerheim, R.; Nitsche, R.; Leo, K. *Appl. Phys. Lett.* **2008**, *93*, 043310.

(20) Swensen, J. S.; Polikarpov, E.; Ruden, A. V.; Wang, L.; Sapochak, L. S.; Padmaperuma, A. B. *Adv. Funct. Mater.* **2011**, *17*, 3250–3258.